Vol. 1, Issue 1, March 2026.
CENTRAL ASIAN TRANSACTIONS ON MATERIALS STRUCTURE AND PROPERTIES

https://doi.org/10.51885/3134-7983_CATMSP_2026_1_8
SRSTI 55.22.23

COMPREHENSIVE EVALUATION OF THE CORROSION, EROSION, AND ABRASION RESISTANCE OF HVOF WC–CO–CR COATINGS ON 30KH13 STEEL

Nazerke Muktanova[1,2*], **Małgorzata Rutkowska-Gorczyca**[3], **Nurtoleu Magazov**[1], **Bauyrzhan Rakhadilov**[2]

[1]NJSC "D. Serikbayev EKTU", Ust-Kamenogorsk, Kazakhstan
[2]PlasmaScience LLP, Ust-Kamenogorsk, Kazakhstan
[3]Wrocław University of Science and Technology, Wrocław, Poland
*Corresponding author: Nazerke Muktanova, e-mail: muktanovan@gmail.com

Keywords:
metal-ceramic coating, HVOF method, erosion, corrosion, abrasion resistance, microstructure, wear resistance

ABSTRACT

This study presents a comprehensive experimental investigation of the corrosion, erosion, and abrasive wear resistance of WC–Co–Cr coatings deposited on 30Kh13 martensitic steel using the high-velocity oxygen-fuel (HVOF) spraying method. Corrosion tests were performed under cyclic salt fog conditions in a 5% NaCl solution, while erosion tests were carried out under the impact of an abrasive particle flow. Abrasive wear was evaluated using a standard method with the calculation of relative wear resistance. The results showed that the WC–Co–Cr coating significantly reduces mass loss and slows the development of corrosion and erosion damage compared with uncoated steel. Under abrasive wear conditions, the relative wear resistance of the coated samples is approximately nine times higher than that of 30Kh13 steel. Microstructural analysis revealed that coating degradation is localized and mainly associated with the destruction of the binder phase. The obtained results confirm the effectiveness of WC–Co–Cr HVOF coatings for protecting parts operating under combined corrosion-mechanical influences.

INTRODUCTION

Intensive wear and corrosion degradation of metallic materials remain one of the key problems in the operation of equipment in the oil and gas, energy, and pumping industries. Working elements such as valves, pump wheels, and gate valves are subjected to the combined effects of abrasive particles, erosive flows, and aggressive corrosive environments (Rao & Mulky, 2023; Gao et al., 2024; Xi et al., 2021; Wang et al., 2019).

Martensitic corrosion-resistant steel 30Kh13 is widely used due to its satisfactory mechanical properties and moderate corrosion resistance. However, under conditions of abrasive erosion and chloride exposure, its operational properties prove to be insufficient, leading to accelerated surface destruction and a reduction in product life (Sola et al., 2013; Scheuer et al., 2019; Xi et al., 2021).

One of the most effective ways to increase wear and corrosion resistance is to apply protective coatings using high-velocity oxygen fuel (HVOF) spraying. This method allows the formation of dense coatings with low porosity, high adhesion, and minimal decarburization of the carbide phase (Sidhu et al., 2005; Sahraoui et al., 2010; Kear et al., 2001; El Rayes et al., 2022).

Among carbide systems, WC–Co–Cr coatings are of particular interest, as the presence of chromium in the binder phase increases corrosion resistance compared to traditional WC–Co coatings, especially in chloride-containing environments (Picas et al., 2019; Magnani et al., 2007; Wang et al., 2019). It has been previously shown that such coatings effectively resist abrasive and erosive wear, but the nature of degradation significantly depends on the spraying parameters, coating thickness, and operating conditions (Sapate et al., 2021).

At the same time, there is insufficient systematic experimental data in the literature comparing the behavior of HVOF WC–Co–Cr coatings and martensitic steels under conditions of corrosion, erosion, and abrasive wear obtained in a single study.

The aim of this work is to conduct a comprehensive study of the corrosion, erosion, and abrasion resistance of WC–Co–Cr coatings applied by the HVOF method to 30Kh13 steel, with a quantitative comparison of their performance characteristics with untreated steel. Particular attention is paid to the kinetics of mass loss, surface morphology, and degradation mechanisms.

MATERIALS AND METHODS

Corrosion-resistant steel 30Kh13 and 86WC-10Co-4Cr coating (further WC-Co-Cr) applied to the surface of this steel were selected as the research materials. Before spraying, the samples were subjected to mechanical processing, degreasing, and abrasive jet cleaning to ensure the required surface roughness. The WC–Co–Cr coating was applied by high-velocity oxygen fuel (HVOF) spraying using commercial 86WC-10Co-4Cr powder with a fraction of 30-40 μm. The spraying distance was 300 mm. Propane was used as fuel, oxygen served as an oxidizer, and air was used to cool the nozzle. The main parameters of the spraying process are given in Table 1.

Table 1. HVOF spraying parameters

№	Propane pressure, bar	Oxygen pressure, bar	Air pressure, bar
HVOF method	2.9	5	3.2
Note – compiled by the authors			

The corrosion resistance of the samples was evaluated using a cyclic salt spray test in a 5% aqueous NaCl solution. One test cycle consisted of exposure to salt spray for 1 hour at a temperature of 25–35 °C, followed by drying of the samples at a temperature of 35 °C for 1 hour. After each cycle, the samples were rinsed with distilled water, dried, and weighed on analytical scales with an accuracy of 0.1 mg. The criteria for assessing corrosion resistance were the loss of sample mass and the appearance of visual signs of corrosion damage to the surface. Erosion resistance tests were conducted at room temperature in accordance with ASTM G76-04. During the experiment, a nozzle with an inner diameter of 5 mm was placed at a distance of 10 mm from the sample surface and oriented perpendicular (at an angle of 90°) to its surface. Quartz sand with a particle size of 50 μm was used as the erosion abrasive. The duration of one exposure cycle was 3 minutes. Before the start of the tests, the samples were weighed on electronic analytical scales with an accuracy of 0.01 mg, after which they were fixed in a holder and exposed to abrasive particles. At the end of the tests, the samples were removed, cleaned in acetone, and reweighed to determine the mass loss due to erosion wear. Samples made of 30Kh13 steel and samples coated with WC–Co–Cr were tested under identical conditions. Abrasive wear resistance was investigated in accordance with GOST 23.208–79. For 30Kh13 steel samples, the tests were carried out at a rotation speed of 600 rpm and a duration of 10 minutes, while for WC–Co–Cr coatings, the modes of 1800 rpm and 30 minutes at a load of 44 N were used. Steel 45 according to GOST 1050-88 in an annealed state with a hardness of 190–200 HV was used as a reference material. The wear resistance of the tested materials was evaluated by comparing their wear with that of the

reference sample. To determine mass loss, the samples were weighed on CRYSTAL 100 CALCE analytical scales with an accuracy of 0.1 mg before and after testing. Mass loss during wear was at least 5 mg. The relative wear resistance of the coatings was calculated based on the data obtained. The surface morphology and microstructure of the cross-sections of the coatings were studied using scanning electron microscopy (SEM) on a SEM3200 instrument equipped with an XFlash Detector 730M-300 (Bruker) energy-dispersive X-ray microanalysis (EDS) system.

All experiments were performed at least three times to ensure the reproducibility of the results.

RESULTS AND DISCUSSION

Figure 1 shows images of the surface of samples with WC–Co–Cr coating and samples of 30Kh13 steel without coating before and after exposure to cyclic salt spray.

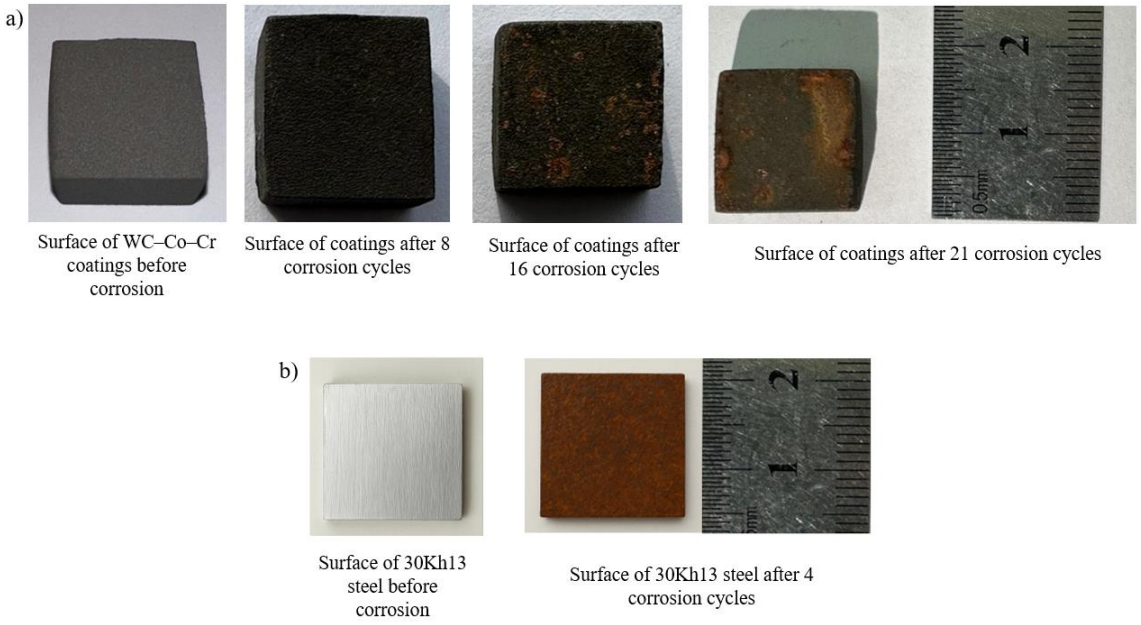

a) sample with 86WC-10Co-4Cr coating; b) sample made of 30Kh13 steel without coating

Figure 1. Surface of test samples before and after corrosion testing in a salt spray chamber

Note – compiled by the authors

The initial state of the WC–Co–Cr coating is characterized by a dense and uniform surface without visible defects. After 8 cycles of corrosion exposure, slight darkening of the surface is observed, with no signs of corrosion. After 16 cycles, local corrosion damage in the form of individual pitting is observed. Further exposure up to 21 cycles leads to more pronounced surface degradation and partial destruction of the coating in certain areas. In contrast to the coated sample, uncoated 30Kh13 steel exhibits low corrosion resistance. As shown in Figure 1b, after only 4 cycles of exposure, pronounced corrosion damage and the formation of rust products are observed, indicating intense degradation of the steel surface in a chloride-containing environment.

The quantitative assessment of corrosion resistance was carried out based on mass loss measurements (Figure 2).

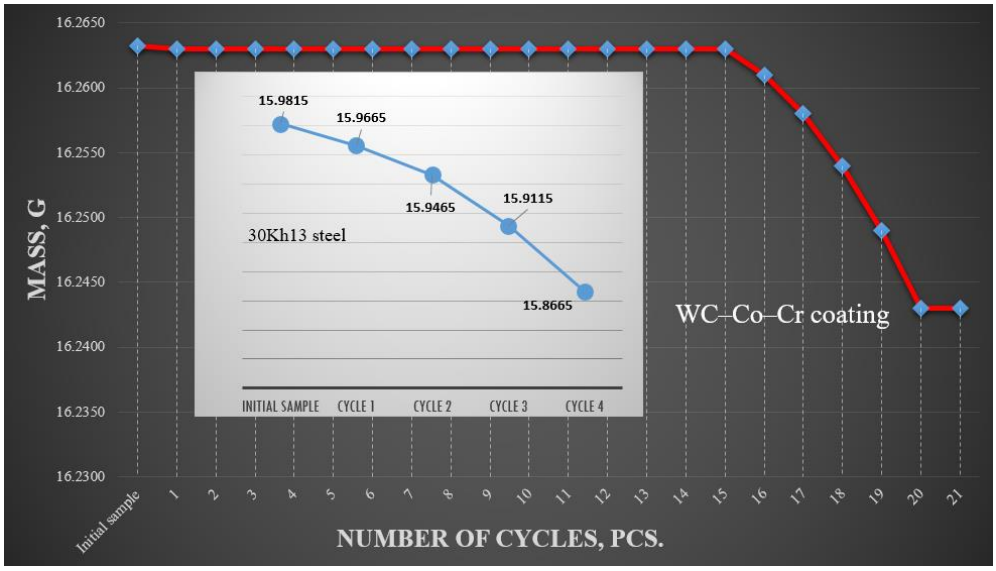

Figure 2. Graph showing the dependence of the mass loss of 30Kh13 steel and 86WC-10Co-4Cr coating on the number of cycles

Note – compiled by the authors

Uncoated 30Kh13 steel samples are characterized by a rapid decrease in mass starting from the first cycle of corrosion exposure. After four cycles, the total mass loss was 115 mg, which corresponds to intensive corrosion destruction of the surface. At the same time, samples with WC–Co–Cr coating retained virtually unchanged mass up to 15 cycles. A noticeable mass loss was recorded only after 16 cycles, and the total mass loss after 21 cycles was 20.2 mg, which is more than five times less than that of untreated steel.

Figure 3 shows a SEM image of the surface of 30Kh13 steel after 4 cycles of corrosion testing in cyclic salt spray conditions, as well as the results of energy-dispersive mapping of the distribution of chemical elements (Fe, Cr, O, Cl, C).

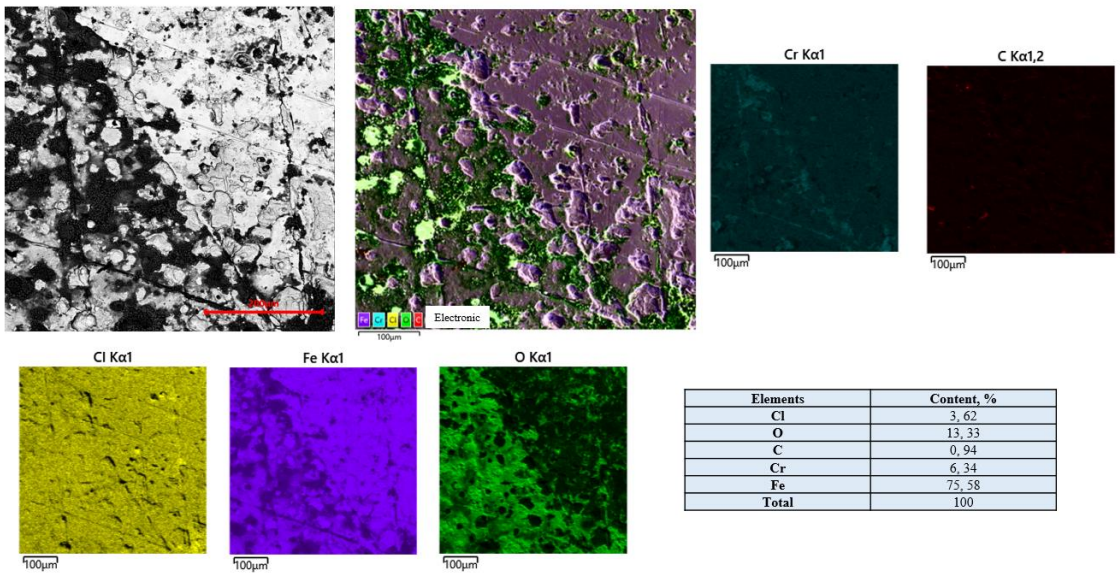

Elements	Content, %
Cl	3, 62
O	13, 33
C	0, 94
Cr	6, 34
Fe	75, 58
Total	100

Figure 3. SEM image of the surface of 30Kh13 steel and the results of elemental mapping after 4 cycles of cyclic salt spray exposure

Note – compiled by the authors

The SEM image shows pronounced localized corrosion damage to the surface, accompanied by the formation of pitting, pores, and areas with corrosion products. Element mapping reveals an increased concentration of oxygen and chlorine in the damaged areas, which indicates the formation of oxide and chloride-containing corrosion products and confirms the development of chloride-induced pitting corrosion. The distribution of iron remains relatively uniform and corresponds to the metal matrix of steel, while the chromium content is reduced, indicating a violation of the passive protective layer under the influence of an aggressive corrosive environment. Quantitative EDS analysis shows a predominance of iron (75.58 wt.%) and the presence of oxygen (13.33 wt.%) and chlorine (3.62 wt.%), confirming intense corrosion oxidation of the surface.

Figure 4 shows SEM images of the surface of the 86WC–10Co–4Cr coating after 21 cycles of corrosion testing in cyclic salt spray conditions: (a) general view of the coating surface, (b) surface areas with marked points for point energy dispersive (EDS) analysis (spectra 1–4).

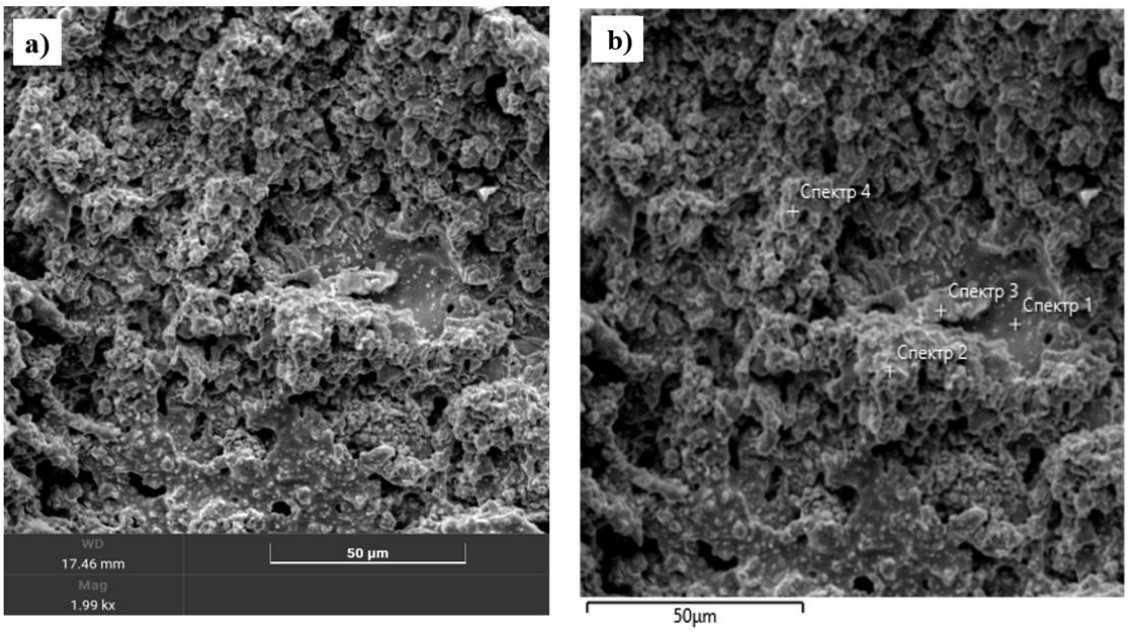

Figure 4. Surface morphology of the 86WC–10Co–4Cr coating (a) and results of point EDS analysis (b) after 21 cycles of cyclic salt spray exposure

Note – compiled by the authors

SEM images show a pronounced micro-relief and porous surface structure formed as a result of corrosion by a chloride-containing environment. Local areas of degradation of the binder phase, pores, and areas of loose corrosion products are observed, indicating the development of selective corrosion of the metal matrix of the coating. The results of point EDS analysis (Figure 4b, Table 2) show variations in elemental composition in different areas of the surface.

Table 2. Results of point EDS analysis of the 86WC-10Co-4Cr coating

Spectrum	O (mass %)	Cr (mass %)	Co (mass %)	W (mass %)
1	3.14	5.38	19.03	72.45
2	13.96	2.94	11.03	72.07
3	8.33	56.49	-	35.18
4	18.59	6.33	10.67	64.40

Note – compiled by the authors

The oxygen content varies in the range of 3.14–18.59 wt.%, reflecting different degrees of surface oxidation. The high mass fraction of tungsten (35.18–72.45 wt.%) confirms the preservation of the WC carbide phase, while fluctuations in the cobalt and chromium content indicate redistribution and partial leaching of the binder phase under the influence of the corrosive environment. The data obtained indicate the localized nature of the corrosion degradation of the coating without signs of its continuous destruction.

Analysis of the cross-section of the 86WC–10Co–4Cr coating using SEM (Figure 5) showed that the coating remains continuous after corrosion exposure, with an average thickness of about 59 μm. In the near-surface zone of the coating, porous areas, local defects, and cracks were observed, spreading mainly from the surface into the depth of the layer, which indicates the development of corrosion degradation under the action of a chloride-containing environment. No significant signs of through-corrosion or delamination of the coating from the substrate were observed.

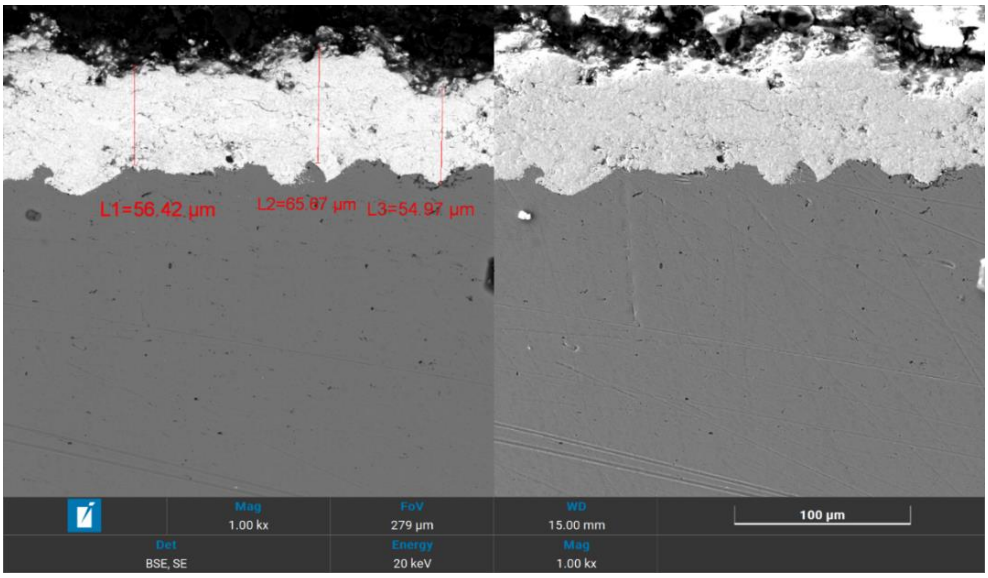

Figure 5. Microstructure of a cross-section of the WC-Co-Cr coating after exposure to a cyclic corrosion test in salt fog

Note – compiled by the authors

Figure 6 shows the results of elemental mapping and linear energy dispersive (EDS) analysis of the cross section of the WC–Co–Cr coating after corrosion testing in cyclic salt spray conditions: (a) distribution maps of the elements W, Co, Cr, Fe, O, and C; (b) profiles of EDS signal intensity changes along the line of analysis crossing the coating and substrate. Element mapping indicates that the compositional integrity of the coating is preserved throughout its thickness, with increased oxygen content localized mainly in the near-surface zone, indicating the development of oxidative processes. Cobalt and chromium signals correspond to the binder phase of the coating and are distributed uniformly throughout the thickness of the layer. Linear EDS analysis shows a sharp decrease in the intensity of the W signal and a simultaneous increase in the Fe signal at the coating-substrate interface, confirming a clear boundary between the layers.

Overall, the results obtained indicate that the application of a WC–Co–Cr coating significantly increases the corrosion resistance of 30Kh13 steel under cyclic salt spray conditions. The coating effectively delays the onset of corrosion damage and reduces the rate of mass loss, despite the development of local degradation of the binder phase during prolonged exposure to an aggressive environment.

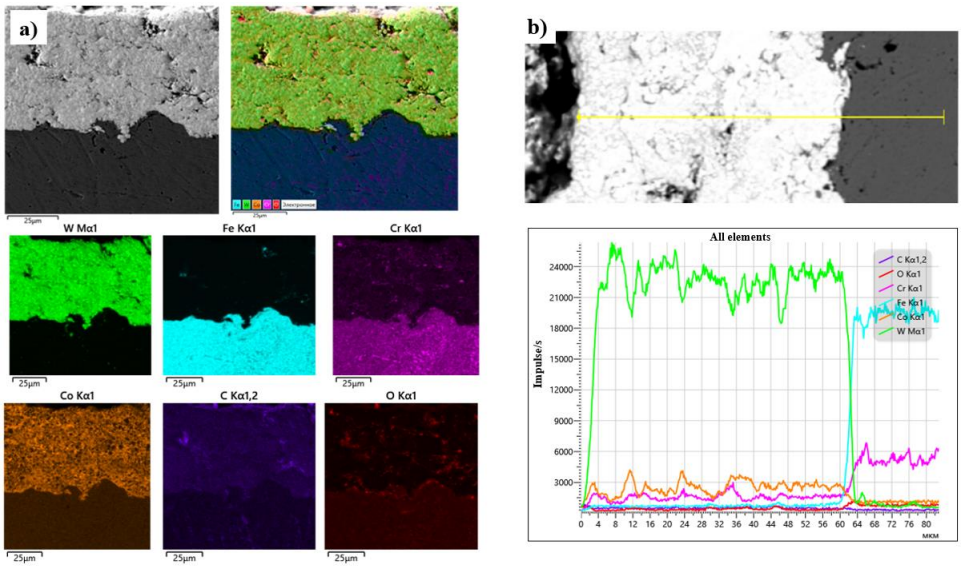

Figure 6. Elemental distribution (a) and linear EDS analysis of the cross-section of the WC–Co–Cr coating (b) after exposure to cyclic salt spray

Note – compiled by the authors

Under real operating conditions, materials and protective coatings are often exposed not only to corrosion but also to erosion caused by the action of solid particle flows. In this regard, for a comprehensive assessment of the operational reliability of 30Kh13 steel and WC-Co-Cr coatings, the next stage of work was to study their erosion resistance under identical test conditions.

Figure 7 shows the evolution of the surface of uncoated 30Kh13 steel during erosion testing. Already after the first cycle, the appearance of a matte zone in the center of the impact area is observed, which indicates the initial stage of abrasive wear. As the number of cycles increases, the eroded area expands and deepens. Starting from the third cycle, a pronounced crater-like depression forms, corresponding to the area of direct impact of abrasive particles. After the sixth cycle, the destruction becomes three-dimensional and is accompanied by significant thinning of the material, indicating high intensity of localized erosion wear.

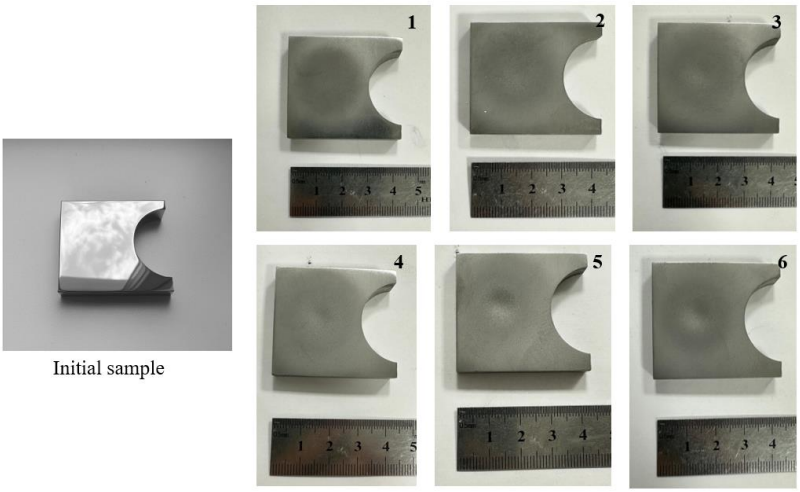

Figure 7. Change in the condition of the surface of uncoated 30Kh13 steel during erosion (cycles 1–6)

Note – compiled by the authors

A quantitative assessment of the erosion damage to 30Kh13 steel was carried out on the basis of cycle-by-cycle mass measurements (Table 3).

Table 3. Change in the mass of 30Kh13 steel during erosion tests

Cycle	Mass, g	Mass loss per cycle, g	Mass loss per cycle, mg
Initial	64, 2477	-	-
Cycle 1	64, 1560	0, 0917	91.7
Cycle 2	64.0512	0.1048	104.8
Cycle 3	63.9156	0.1356	135.6
Cycle 4	63.7109	0.2047	204.7
Cycle 5	63, 4013	0.3096	309.6
Cycle 6	63.0012	0.4001	400.1
Note – compiled by the authors			

The total mass loss after six cycles was 1.2465 g, which corresponds to approximately 1.94% of the initial mass of the sample. The nature of the mass change indicates progressive and accelerating wear, especially after the fourth cycle, when mass loss exceeds 200 mg per cycle. The data obtained indicate low erosion resistance of 30Kh13 steel under the specified test conditions.

To increase erosion resistance, a coating of 86WC–10Co–4Cr was applied to the surface of 30Kh13 steel using high-velocity oxygen fuel (HVOF) spraying. The average thickness of the formed coating was about 360 μm. The sequence of changes in the coating surface during erosion testing is shown in Figure 8.

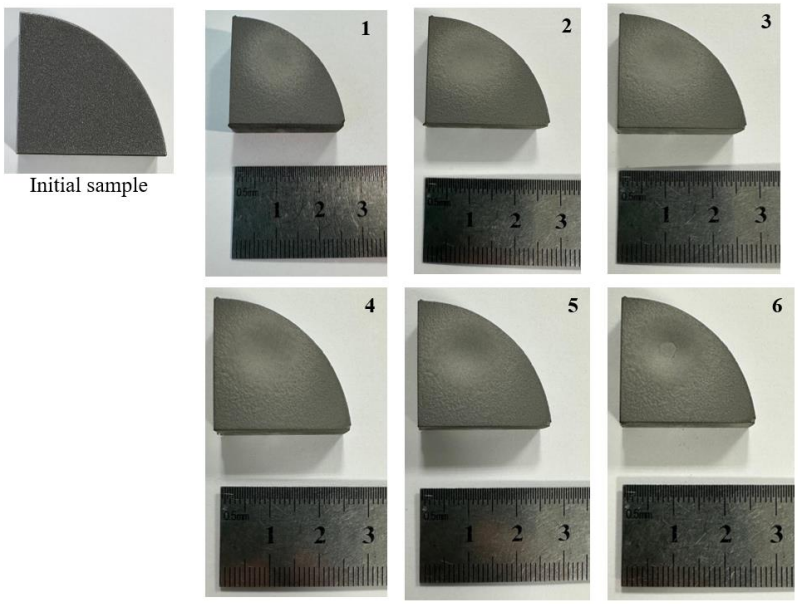

Figure 8. Changes in the surface of the 86WC-10Co-4Cr coating after each of the six cycles of erosion exposure

Note – compiled by the authors

At all stages of testing, three characteristic zones are clearly visible on the surface: a central zone of intense erosion, a zone of moderate wear, and a peripheral area with minimal damage.

Cycle-by-cycle weighing of coated samples (Table 4) showed that in the first four cycles, the mass loss increased relatively smoothly and did not exceed 121.6 mg per cycle.

Table 4. Change in mass of the WC-Co-Cr coated sample during erosion testing

Cycle	Mass, g	Mass loss per cycle, g	Mass loss per cycle, mg
Initial	31.4067	-	-
Cycle 1	31, 3412	0, 0655	65.5
Cycle 2	31, 2511	0.0901	90.1
Cycle 3	31, 1452	0.1059	105.9
Cycle 4	31, 0236	0.1216	121.6
Cycle 5	30.8213	0.2023	202.3
Cycle 6	30, 5200	0.3013	301.3
Note – compiled by the authors			

A significant increase in mass loss is observed after the fifth cycle, accompanied by a sharp deterioration in the surface condition, indicating the destruction of the binder phase and partial breakdown of the coating. In the sixth cycle, local exposure of the substrate is recorded, confirmed by an increase in mass loss to 301.3 mg. The total mass loss of the coated sample after six cycles was 0.8867 g (2.82% of the initial mass). Although the relative mass loss of the coating is comparable to that of steel, the nature of the wear is fundamentally different. The WC–Co–Cr coating effectively inhibits erosion damage in the initial and intermediate stages of exposure, while the sharp acceleration of wear is associated with the protective layer reaching a critical state and the abrasive reaching the substrate.

A comparative analysis of the mass loss curves (Figure 9) shows that uncoated samples are characterized by significantly more intense erosion wear, especially starting from the fourth cycle. At the same time, the WC–Co–Cr coating provides a smoother mass change and delays the development of intense erosion damage.

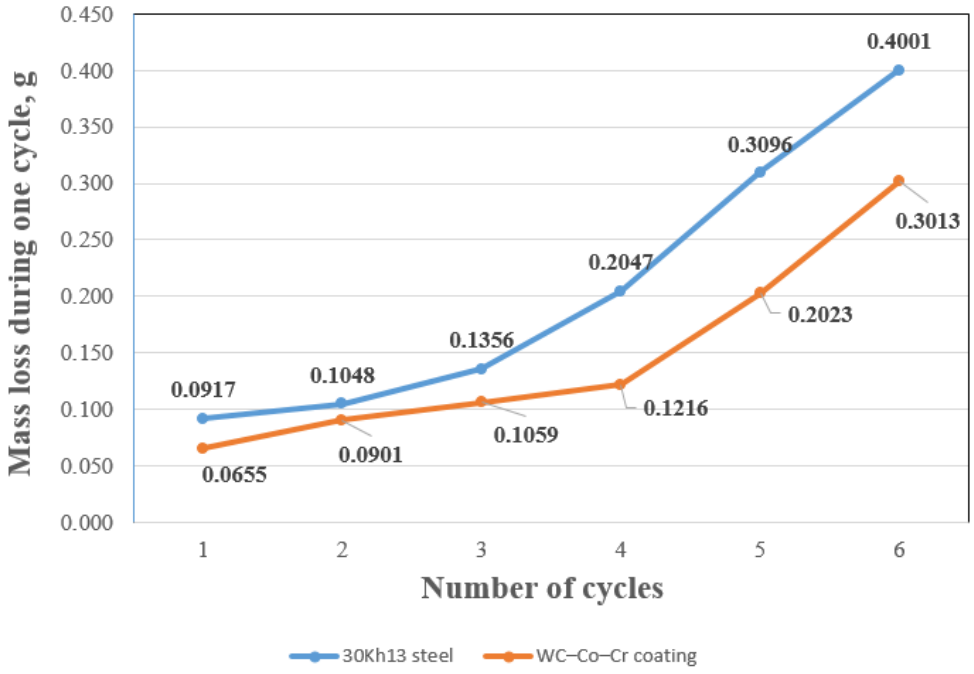

Figure 9. Graph of mass loss of samples with and without WC-Co-Cr coating depending on the number of erosion cycles

Note – compiled by the authors

Thus, the results of erosion tests confirm that the application of a WC–Co–Cr coating significantly increases the erosion resistance of 30Kh13 steel, especially in the early and intermediate stages of exposure to abrasive particles.

In addition to erosion wear, abrasive wear caused by prolonged contact of the surface with hard particles has a significant impact on the durability of parts. Figure 10 shows the results of weighing the samples before the abrasion tests, recording their initial mass.

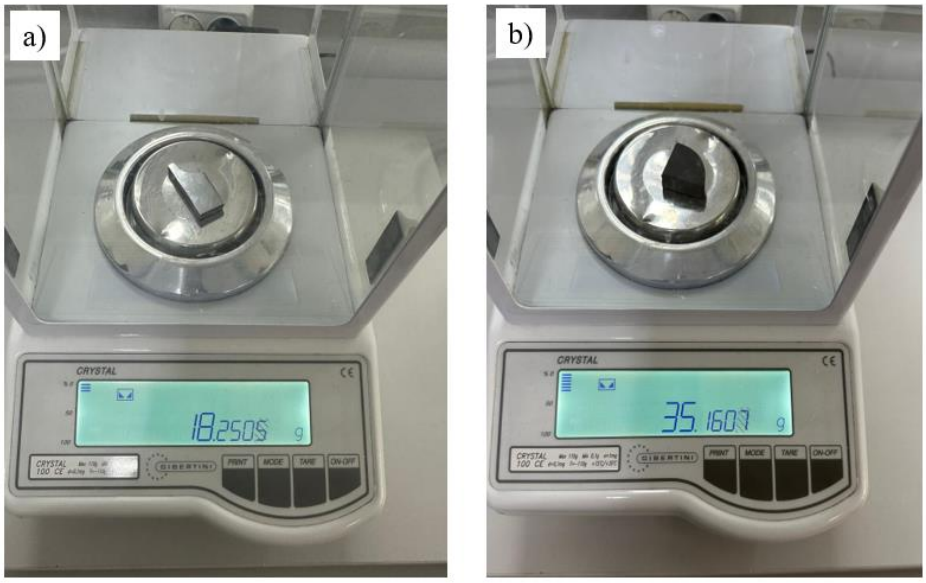

a) 30Kh13 steel; b) sample with 86WC-10Co-4Cr coating

Figure 10. Weighing of samples before testing

Note – compiled by the authors

The initial mass of the 30Kh13 steel sample was 18.2505 g, while the mass of the sample with WC–Co–Cr coating was 35.1607 g. These values were used as initial values in the subsequent determination of mass loss during wear. The appearance of the samples after abrasion testing is shown in Figure 11.

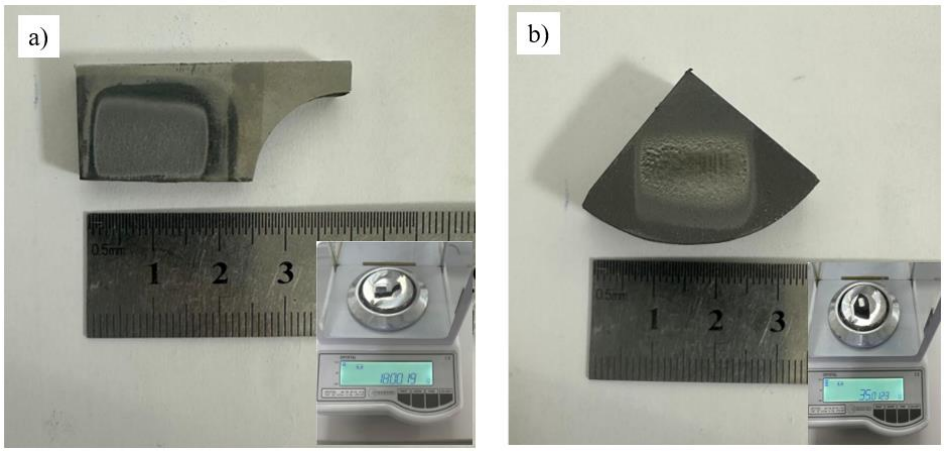

a) 30Kh13 steel; b) sample with 86WC-10Co-4Cr coating

Figure 11. Samples after abrasive wear testing

Note – compiled by the authors

Steel 30Kh13 is characterized by the formation of a more extensive and pronounced wear zone, while in the sample with a WC–Co–Cr coating, the wear zone is smaller and more localized. The quantitative results of the abrasion tests are given in Table 5.

Table 5. Results of abrasive wear tests on samples

No.	Sample	Test time, min	Mass before testing *m*, g	Mass after testing *m*, g	Mass loss, g
1	Steel 30Kh13	10	18.2505	18.0019	0.2486
2	WC-Co-Cr coating	30	35.1607	35.0123	0.1484
Note – compiled by the authors					

It was found that 30Kh13 steel is characterized by the greatest loss of mass, despite the shorter duration of exposure. At the same time, the sample with a WC–Co–Cr coating demonstrates a significantly lower loss of mass even with a longer test time, which indicates a higher resistance of the coating to abrasive wear. For a comparative assessment of wear resistance, the relative wear resistance K_i was calculated using formula (1), which takes into account mass loss, material density, and test conditions:

$$K_{\text{i}} = \frac{g_{\text{e}}\rho_{\text{i}}N_{\text{i}}}{g_{\text{i}}\rho_{\text{e}}N_{\text{e}}} \quad (1)$$

where g – is the mass loss, ρ – is the material density, N – is the number of revolutions, and the indices "e" and "i" correspond to the reference and test materials.

The results of the relative wear resistance calculation are presented in Table 6.

Table 6. Results of calculations of relative wear resistance (K_i) of the tested samples to abrasive wear

No.	Sample name	Mass loss g_i, g	Density ρ, g/cm^{3*}	Relative wear resistance K_i
1	Steel 30Kh13	0.2486	7.67	0.2
2	WC-Co-Cr coating	0.1484	14.5	1.8
3	Steel 45 (reference)	0.048	7.8	1
Note – compiled by the authors				

It has been established that for 30Kh13 steel, the value of K_i is 0.2, while for the WC–Co–Cr coating, this indicator reaches 1.8. The reference sample made of 45 steel is taken as a unit. Thus, the application of the WC–Co–Cr coating provides an increase in relative abrasive wear resistance by approximately 9 times compared to uncoated 30Kh13 steel.

Thus, the test results confirm that the WC–Co–Cr coating effectively increases the resistance of 30Kh13 steel to abrasive wear. Together with the data on corrosion and erosion resistance, this indicates the advisability of using these coatings to protect parts operating under combined corrosion, erosion, and abrasion conditions.

CONCLUSION

1. It has been shown that applying a WC–Co–Cr coating using the HVOF method significantly increases the corrosion resistance of 30Kh13 steel in cyclic salt spray conditions. The mass loss of coated samples is more than five times lower than that of uncoated steel, and the onset of intensive corrosion degradation is significantly delayed.

2. It has been established that during corrosion, the degradation of the coating is localized and is mainly associated with the oxidation and selective corrosion of the Co–Cr binder phase, while the WC carbide phase remains relatively stable.

3. The results of erosion tests showed that the WC–Co–Cr coating effectively reduces the intensity of erosion wear of 30Kh13 steel at the initial and intermediate stages of exposure to abrasive particles. Accelerated coating destruction is observed when the protective layer reaches a critical degree of thinning and the abrasive reaches the substrate.

4. Under conditions of abrasive wear, the WC–Co–Cr coating provides a significant increase in wear resistance: the relative wear resistance of coated samples exceeds that of 30Kh13 steel by approximately 9 times.

CONFLICT OF INTEREST: The authors declare no conflict of interest.

FUNDING: This study was funded by the Committee of Science of the Ministry of Science and Higher Education of the Republic of Kazakhstan (Grant number: BR24992854).

STATEMENT ON THE USE OF ARTIFICIAL INTELLIGENCE TECHNOLOGIES: Authors confirm that no artificial intelligence (AI) tools were used in the preparation of this scientific article. All stages of the work, including writing, editing, fact-checking, and data analysis, were carried out independently by the authors.

REFERENCES

Rao, P., & Mulky, L. (2023). Erosion-corrosion of materials in industrial equipment: a review. ChemElectroChem, 10(16), e202300152. https://doi.org/10.1002/celc.202300152

Lyphout, C., et al. (2013). Tungsten carbide deposition processes for hard chrome alternative: Preliminary study of HVAF vs. HVOF thermal spray processes. Proceedings of the International Thermal Spray Conference (ITSC 2013), 506–511. ASM International. https://doi.org/10.31399/asm.cp.itsc2013p0506

Sidhu, T. S. N., Prakash, S., & Agrawal, R. D. (2005). State of the art of HVOF coating investigations—A review. Marine Technology Society Journal, 39(2), 53–64. https://doi.org/10.4031/002533205787443908

Gao, G., Guo, S., & Li, D. (2024). A review of cavitation erosion on pumps and valves in nuclear power plants. Materials, 17(5), 1007. https://doi.org/10.3390/ma17051007

Xi, Y., et al. (2021). Improvement of erosion–corrosion behavior of AISI 420 stainless steel by ion-assisted deposition ZrN coatings. Metals, 11(11), 1811. https://doi.org/10.3390/met11111811

Sola, R., et al. (2013). Effect of quenching method on the wear and corrosion resistance of stainless steel AISI 420 (Type 30Kh13). Metal Science and Heat Treatment, 54(11–12), 644–647. https://doi.org/10.1007/s11041-013-9543-4

Scheuer, C. J., et al. (2019). AISI 420 martensitic stainless steel corrosion resistance enhancement by low-temperature plasma carburizing. Electrochimica Acta, 317, 70–82. https://doi.org/10.1016/j.electacta.2019.05.135

Sahraoui, T., et al. (2010). HVOF sprayed WC–Co coatings: Microstructure, mechanical properties and friction moment prediction. Materials & Design, 31(3), 1431–1437. https://doi.org/10.1016/j.matdes.2009.09.031

Kear, B. H., Skandan, G., & Sadangi, R. K. (2001). Factors controlling decarburization in HVOF sprayed nano-WC/Co hardcoatings. Scripta Materialia, 44(8–9), 1703–1707. https://doi.org/10.1016/S1359-6462(01)00789-0

Seitov, B., et al. (2025). Review of physical and mechanical properties, morphology, and phase structure in Cr_3C_2–NiCr composite coatings sprayed by HVOF method. Coatings, 15(4), 479. https://doi.org/10.3390/coatings15040479

El Rayes, M. M., Sherif, E. S. M., & Abdo, H. S. (2022). Comparative study into microstructural and mechanical characterization of HVOF WC-based coatings. Crystals, 12(7), 969. https://doi.org/10.3390/cryst12070969

Picas, J. A., et al. (2019). Corrosion mechanism of HVOF thermal sprayed WC–CoCr coatings in acidic chloride media. Surface and Coatings Technology, 371, 378–388. https://doi.org/10.1016/j.surfcoat.2018.11.090

Wang, H., et al. (2019). Corrosion resistance enhancement of WC cermet coating by carbides alloying. Corrosion Science, 147, 372–383. https://doi.org/10.1016/j.corsci.2018.11.021

Magnani, M., et al. (2007). WC–CoCr coatings sprayed by high velocity oxygen-fuel (HVOF) flame on AA7050 aluminum alloy: Electrochemical behavior in 3.5% NaCl solution. Materials Research, 10, 377–385. https://doi.org/10.1590/S1516-14392007000400008

Sapate, S. G., et al. (2021). Effect of coating thickness on the slurry erosion resistance of HVOF-sprayed WC-10Co-4Cr coatings. Journal of Thermal Spray Technology, 30(5), 1365–1379. https://doi.org/10.1007/s11666-021-01206-6

Information about authors

Nazerke Muktanova– doctoral student of the specialty "Technical Physics", East Kazakhstan Technical University named after D. Serikbaev, Ust-Kamenogorsk, Kazakhstan,
e-mail: muktanovan@gmail.com,
ORCID: https://orcid.org/0000-0002-4823-6640,

Małgorzata Rutkowska-Gorczyca – Doctor of Technical Sciences, Department of Automotive Engineering, Wrocław University of Science and Technology, Wrocław, Poland,
e-mail: malgorzata.rutkowska-gorczyca@pwr.edu.pl,
ORCID: https://orcid.org/0000-0003-2712-5914,

Nurtoleu Magazov – doctoral student of the specialty "Technical Physics", East Kazakhstan Technical University named after D. Serikbaev, Ust-Kamenogorsk, Kazakhstan,
e-mail: magazovn@gmail.com,
ORCID: https://orcid.org/0000-0002-9941-9199,

Bauyrzhan Rakhadilov – Doctor of Technical Sciences, Professor, General Director of PlasmaScience LLP, Ust-Kamenogorsk, Republic of Kazakhstan,
e-mail: rakhadilovb@mail.ru,
ORCID: https://orcid.org/0000-0001-5990-7123